

Discrete Element Method Study of Shear Wave Propagation in Granular Soil

Étude de la propagation des ondes de cisaillement dans un sol granuleux par la méthode des éléments discrets

Ning Z.

Department of Civil, Construction, and Environmental Engineering, North Carolina State University, Raleigh, NC, USA

Evans T.M.

School of Civil & Construction Engineering, Oregon State University, Corvallis, OR, USA

ABSTRACT: Shear wave velocity is a fundamental parameter for describing the small-strain response of soil and is a critical input for multiple constitutive models used to describe the static and dynamic behavior of granular materials. Shear wave velocity is understood to be a function of particle parameters (shape, elastic properties, gradation) and state (void ratio, boundary stress), but the exact effects of these parameters are difficult to measure using laboratory results alone. This paper presents results of a study of shear wave propagation in granular soil using the discrete element method (DEM). In this study, cylindrical assemblies of particles were subjected to shear wave excitation at one end and axial propagation velocities were measured. The effects of excitation frequency, particle size, and confining stress were investigated. Micromechanical observation of the specimen is presented and analyzed in terms of particle velocity vectors.

RÉSUMÉ : La célérité de l'onde de cisaillement est un paramètre fondamental pour décrire le modèle constitutif du sol. Plusieurs modèles utilisent ce paramètre pour décrire le comportement statique et dynamique de matériaux granuleux. La vitesse de l'onde de cisaillement est fonction des paramètres des particules (la forme, les propriétés élastiques, la granularité) et de leur état (indice des vides, contrainte aux limites). Par contre, il est difficile de mesurer l'effet exact de ces paramètres en utilisant des résultats expérimentaux. Cet article présente les résultats de l'étude de la propagation de l'onde de cisaillement dans un sol granuleux en utilisant la méthode des éléments discrets. Les particules, groupées en cylindre, sont excitées par des ondes de cisaillement à un bout du cylindre. Les vitesses de propagation sont ensuite mesurées. Les effets de la fréquence d'excitation, de la taille des particules et de la contrainte de confinement sont étudiés. Les observations du spécimen sont présentées et analysées en termes de vecteurs de célérité des particules.

KEYWORDS: small strain, shear wave velocity, discrete element method.

1 INTRODUCTION

Shear (S-) wave velocity is a fundamental parameter for describing the small-strain response of soil and is a critical input for multiple constitutive models used to describe the static and dynamic behavior of granular materials (Santamarina 2001). S-wave velocity is understood to be a function of particle parameters (e.g. shape, elastic properties, gradation) (Patel et al. 2009) and state (e.g. void ratio, boundary stress) (Hardin and Richart 1963). Many of these properties can be measured (or observed) as specimen-averaged quantities, but in some cases, the parameter of interest is not directly observable using standard laboratory practices. For example, Agnolin and Roux (2007) have shown that shear wave velocity is a function of both void ratio (packing fraction) and coordination number (i.e., specimens with identical void ratios but different coordination numbers exhibit different wave propagation speeds). This complex behavior implies a need for investigation of wave propagation in particulate assemblies that goes beyond traditional specimen-averaged approaches.

Discrete element method (DEM) simulations are a useful tool for investigating the complex behavior of particulate materials in conjunction with laboratory tests. In terms of wave propagation, 2D DEM simulations have been conducted to study the general relationships between wave propagation variables and soil fabric (Sadd et al. 1993). In a DEM study of the acoustic properties of weakly cemented sandstone by Li and Holt (2002), a logic similar to S-wave generation and measurement in laboratory tests was applied. O'Donovan et al.

(2012) recently used 2D DEM models to simulate bender element tests on an idealized granular material.

In the current study, 3D DEM simulations were used to simulate S-wave propagation in a granular material. The effects of excitation frequency, particle size and confining stress are investigated and compared to published trends of small-strain response for granular materials. Micromechanical observation of the specimen is presented in terms of particle velocity vectors.

2 SIMULATION OF SHEAR WAVE PROPAGATION

2.1 Generation of DEM assembly and shear waves

Cylindrical DEM specimens were generated with the following properties: $G_s=2.7$, $D_{50}=2.0$ mm, $C_u=1.2$, $G_g=2.9$ GPa, $v_g=0.31$, and $\mu=0.31$ (note that G_g , v_g , and μ are grain, not specimen, parameters). Two planar rigid walls defined the top and bottom boundaries of the specimen and were used to control the applied vertical stress. Radial confinement was supplied by stacked cylindrical walls (Zhao and Evans, 2009) to simulate a flexible membrane, which can help to minimize the wave reflection from the lateral boundaries (O'Donovan et al. 2012).

S-waves were generated by applying a horizontal excitation to a thin layer of particles at one end of the specimen using a sinusoidal pulse. Compared to the S-wave generation method used in the bender element test, in which the wave source is a point and the wave propagation front is spherical, the S-wave generation method in the current study can help to reduce the compression (P) wave interference effect (Lee and Santamarina

2005) observed in physical specimens. In DEM simulations the displacement and velocity of each individual particle can be monitored, allowing for the specification of multiple wave receivers at arbitrary locations. Figure 1 shows five particles along the central axis of the cylindrical specimen that were selected as S-wave receivers.

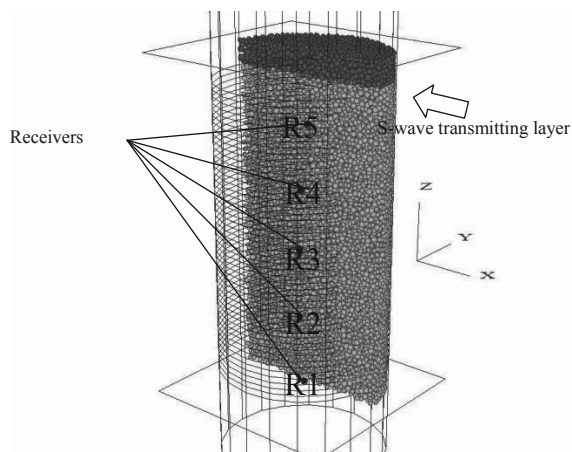


Figure 1. A DEM specimen with S-wave transmitting layer and receivers (for clarity, only half of the specimen is shown).

2.2 Interpretation of travel time

Accurate determination of signal travel time has been the subject of considerable research in laboratory S-wave velocity measurements (e.g., Styler and Howie 2012). Many factors, such as cross-talk between the source and the receiver (Lee and Santamarina 2005), system delay (Yang and Gu 2012), fabrication defects in the testing device (Montoya et al. 2012), and electric and environmental noise add to the uncertainties and the difficulties in the interpretation of receiving signal.

In DEM simulations, most of these aforementioned influence factors can be eliminated. Figure 2 shows 'clean' source and receiving signals from a typical DEM S-wave propagation simulation. The amplitude of the signal is a representation of the displacement of particles in the direction of the excitation (along x-axis in Figure 2). It can be seen that the receivers' respond to the excitation at different times. The delays of the first arrival between equally spaced receivers are almost the same. The receiving signals have identical wave forms but attenuate as the distance to the source increases.

In laboratory, S-wave velocity is typically calculated from the travel time and the distance between wave transmitter and receiver, while in DEM simulations it is also possible to calculate S-wave velocity between the receivers. The common start-to-start and peak-to-peak methods can be applied between source and receiver and between any two receivers. In simulation, when applying the cross-correlation method (Viggiani and Atkinson 1995) between receiving signals, it is expected to be 'cleaner' to interpret compared to laboratory data because they contain less noise and there is a very high similarity between the waveforms.

In the bender element test, the wave motion is indirectly expressed in the change of voltage, which means that the initial polarization between the input and the output signal does not necessarily reflect the relative direction of wave motions at the wave source and at the receiver. It is for the reason that the polarity of the signal is not only determined by the direction that the bender element curves but also affected by the wiring of the bender element electrodes. Unlike in the bender element test, the polarity of the signal in the current simulations directly represents the direction of wave motion, which helps to identify whether the initial deflection of the receiving signal is caused by the S-wave (which results in the same polarity as the source

signal) or by the P-wave reflected from the side boundaries (which results in an inverse polarity of the source signal). From Figure 2, it can be seen that the initial deflection of the receiving signals has the same polarity as the source signal, which indicates little P-wave interference to the first arrival of the receiving signal. The S-wave velocities shown in this manuscript were determined as follows: the travel times between the source layer and the two far most receivers (to avoid near-field effects; Sanchez-Salineró et al. 1986) were determined by the start-to-start method; second, the final representative S-wave velocity was determined by averaging the travel times obtained in step one.

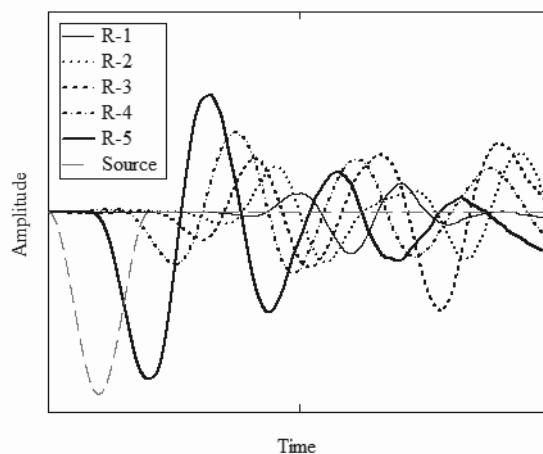


Figure 2. Source signal and receiving signals from a typical DEM S-wave propagation simulation ($D_{50} = 2.0$ mm; $e = 0.63$; $\sigma'_3 = 150$ kPa. Note: for clarity, the amplitudes of the receiving signals are upscaled to facilitate comparison)

3 EFFECTS OF EXCITATION FREQUENCY

In bender element tests, the response of the receiver bender element is enhanced when the frequency of the input signal approaches the resonant frequency of the bender element-soil system (Lee and Santamarina 2005). The resonant frequency can be determined in the laboratory by sweeping the excitation frequency of a sine pulse. The DEM models were excited by sine pulse with different frequencies to approximately identify the resonant frequency. Figure 3 shows the response from one of the receivers in a DEM specimen excited by sine pulse signals with a frequency range from 1 kHz to 100 kHz.

From Figure 3 it is apparent that the response of the receiver is rather weak under excitation frequencies of 1 kHz and 2 kHz. The strongest response is achieved at 5 kHz. Thus, the resonant frequency is located in the range 2-10 kHz. This agrees with published laboratory findings (Santamarina and Fam 1997). The response signals are strong with similar waveform across a wide range of excitation frequencies from 5 kHz to 100 kHz.

Frequency domain analyses were also used to investigate the effect of excitation frequency (Figure 4). It can be seen that the highest amplitude occurs at around 3 kHz, consistent with the observations from time domain analyses. Figure 4 also shows that the receiving signal contains a range of frequency components though the transmitted signal is a sine pulse. When the frequency of the transmitted signal is lower than the resonant frequency (3 kHz), the predominant frequency of the corresponding receiving signal is identical to the frequency of the transmitted signal. However, when the frequency of the transmitted signal is higher than the resonant frequency, the predominant frequency of the corresponding receiving signal is roughly equal to the resonant frequency. The DEM specimen works as a low-pass filter, rejecting frequency components higher than the cut-off frequency, which is found to be the resonant frequency discussed above. The analytical illustration of this low-pass filtering effect in discrete media can be found

in the work by Santamarina (2001). This phenomenon was also reported by Yang and Gu (2012) in their experimental study.

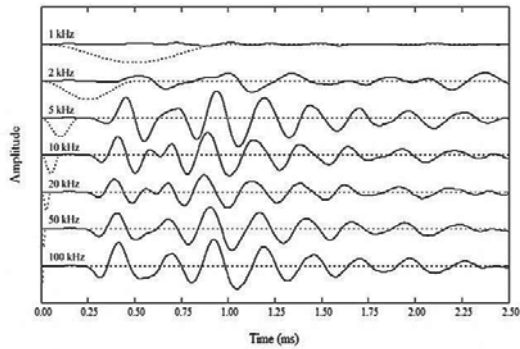


Figure 3. Response of a receiver in the time domain, excited by a sine pulse with different frequencies ($D_{50} = 2.0$ mm; $e = 0.63$; $\sigma'_3 = 150$ kPa. Note: for clarity, the scale of the magnitude for the source signal and the receiving signals are different)

Because the materials with internal spatial scales are inherently dispersive (Santamarina 2001), wave propagation velocity varies with frequency in granular soils. There are experimental studies (Blewett et al. 2000; Styler and Howie 2012) showing frequency-dependent S-wave velocity responses. In the 2D DEM simulation by O'Donovan et al. (2012), the S-wave velocity increases linearly with the transmitted frequency.

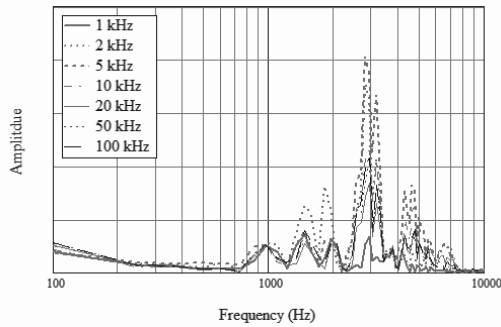


Figure 4. Response of receiver in frequency domain, excited by sine pulse with different frequencies ($D_{50} = 2.0$ mm; $e = 0.63$; $\sigma'_3 = 150$ kPa).

Figure 3 shows that the variation of the first arrival of the S-wave can be observed, though it is not obvious. The S-wave velocity increases slightly (from 220 m/s to 231 m/s) when the transmitted frequency increases from 1 kHz to 5 kHz. This is attributed to the viscous damping effect at the inter-particle contacts (O'Donovan et al. 2012). When the transmitted frequency is higher than the resonant frequency, the variation of S-wave velocity becomes even less appreciable (a consequence explained by the aforementioned low-pass filter effect).

4 PARTICLE SIZE AND CONFINING STRESS EFFECTS

The effect of particle size on S-wave velocity has been widely studied by using bender element tests. A recent work by Yang and Gu (2012) found controversial results by comparing many previous researches. DEM simulation allows for the study of particle size effect with a much larger size range than physical test does. Knowing the particle size effects on wave propagation problem is also important for DEM simulation to determine whether the mass-scaling (O'Sullivan, 2011) is applicable. Three mean particle sizes were considered (2 mm, 20 mm, 200 mm). Since wave propagation involves high frequency effects, different responses are expected from models with different particle sizes. Figure 5 shows the effects of particle size on S-wave velocity and resonant frequency. There was little change in S-wave velocity over three orders of magnitude in particle

size. This agrees with Yang and Gu (2012), who found that S-wave is effectively size independent. Regarding the resonant frequency of model, a linearly decreasing trend with the particle size was observed.

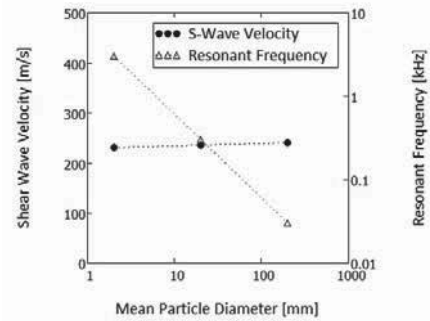


Figure 5. Effects of particle size on S-wave velocity and resonant frequency ($D_{50} = 2$ mm, 20 mm, 200 mm; $e = 0.62-0.63$; $\sigma'_3 = 150$ kPa)

These results indicate that mass-scaling (e.g. by manipulating the particle size; Evans and Frost 2007, Jacobson et al. 2007, Belheine et al. 2010) can be applied to reduce computing time in DEM simulations of S-wave propagation. The excitation frequency should be carefully selected near the resonant frequency (a function of the particle size) to obtain strong frequency response in the model.

Stress state affects interparticle stiffness (Santamarina 2001) and, perhaps more significantly, contact quality (Evans et al. 2011) and thus, wave propagation speed. Many empirical relationships between S-wave velocity and effective confining stress have been proposed (Hardin and Richart 1963) for sands. One general form is as follows:

$$V_s = \alpha \cdot \left(\frac{\sigma'}{1 \text{ kPa}} \right)^\beta \quad (1)$$

where α and β are fitting parameters and σ' is the effective confining stress in kPa.

In this study, the S-wave velocities of a DEM specimen with $D_{50} = 2.0$ mm were determined under confining stresses ranging from 50 to 900 kPa. The simulation results present a similar trend as observed in the lab as shown in Figure 6. The fitting parameters α and β were found to be 95.5 and 0.18 respectively, which fall into the range of typical values for sand and OC clay (Fernandez 2000)

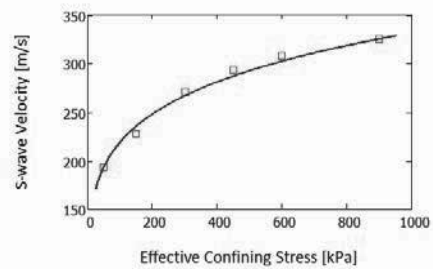


Figure 6. Effects of confining stress on S-wave velocity ($D_{50} = 2.0$ mm; $e = 0.62-0.63$)

5 MICROMECHANICAL OBSERVATIONS

In laboratory tests, it is not possible to directly observe complex wave motions within the specimen. DEM simulations allow for micromechanical predictions of material response, which can help to provide a better understand of the complexity of wave propagation mechanisms in granular materials. Observations of the particle velocity vectors are briefly considered below.

Figure 7 shows particle velocity vectors on three specific cutting planes of a DEM specimen 10 ms after excitation. The cutting plane on the left goes through the central axis of the specimen with its normal parallel to Y-axis. The cutting plane 1-1 and the cutting plane 2-2 are at the height of two receivers respectively with their normal parallel to Z-axis. The particle

velocity vectors on these cutting planes show dominant S-wave motions (from right to left) in the central part of the specimen while minor P-wave motions developed on the sides (with the particle on the right moving downwards and the particle on the left moving upwards). Though the P-waves travel faster, they cause little interference at the central part of the specimen where the receivers are located. At the time shown in Figure 7, the S-wave front just passes cutting plane 1-1 but has not yet reached cutting plane 2-2. A significant amount of additional particle level information is available from DEM simulations, including displacement vectors, contact forces, and contact slip. This information is being analyzed as part of ongoing studies into the fundamental nature of shear wave propagation in granular assemblies.

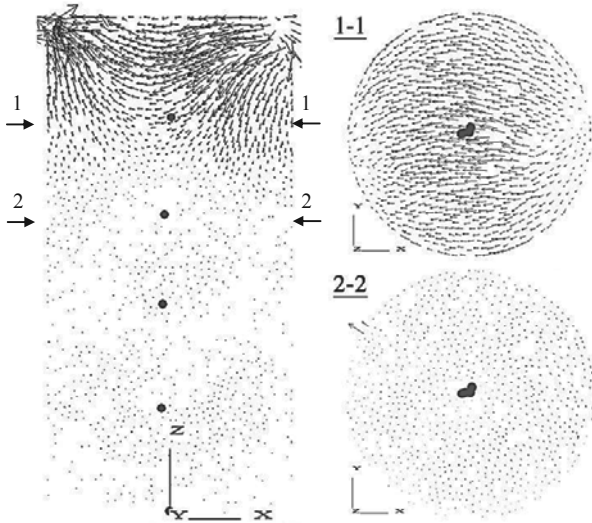


Figure 7. Particle velocity vectors on different cutting planes of a DEM specimen at a 10ms time point after excitation

6 CONCLUSION

This paper presents a DEM study of S-wave propagation in random assemblies of spherical particles. DEM simulations provide high quality receiving S-wave signals, given that the response is free of factors such as cross-talk, system delay, and environmental noise. A multiple receiver setup allows for more reliable S-wave velocity determination.

Excitation frequency showed significant impact on the response of specimen. Similar to laboratory observations, a resonant frequency that resulted in the strongest response was identified in DEM simulations. The granular specimen functioned as a low-pass filter when excited by a sine pulse with different frequencies. Frequency components that were higher than the resonant frequency were significantly attenuated. Dispersion was observed when the excitation frequencies were low. The affect of excitation frequency on S-wave velocity became less appreciable when the frequencies were higher than the resonant frequency.

Particle size had less of an impact on S-wave velocity while the resonant frequency presented an inverse linear relationship with particle size. Mass scaling can be applied in DEM wave-propagation simulation in terms of S-wave velocity analysis when the transmitted frequency is selected appropriately.

The S-wave velocity increased with increasing effective confining stress, and is described by an empirical formula previously developed based on laboratory tests. The fitting parameters obtained in this DEM simulation were similar to those for sands and OC clays measured in the lab.

Velocity vectors highlighted the complex motions of individual particles during wave propagation. They showed dominant S-wave motion along the central area of the specimen along with minor P-wave motion on the sides.

7 REFERENCES

- Agnolin, I., and Roux, J. (2007). "Internal states of model isotropic granular packings. III. Elastic properties." *Physical Review E - Statistical, Nonlinear, and Soft Matter Physics*, 76(6).
- Belheine, N., Plassiard, J. -, Donze, F. -, Darve, F., and Seridi, A. (2009). "Numerical simulation of drained triaxial test using 3D discrete element modeling." *Comput. Geotech.*, 36(1-2), 320-331.
- Blewett, J., Blewett, I. J., and Woodward, P. K. (2000). "Phase and amplitude responses associated with the measurement of shear-wave velocity in sand by bender elements." *Can. Geotech. J.*, 37 1348-1357.
- Evans, T. M., and Frost, J. D. (2007). "Shear banding and microstructure evolution in 2D numerical experiments." *Geo-Denver 2007: New Peaks in Geotechnics*, February 18, 2007 - February 21, American Society of Civil Engineers, Denver, CO, United States, 28.
- Evans, T.M., T.S. Yun, and J.R. Valdes. (2011). "Effective Thermal Conductivity in Granular Mixtures: Numerical Studies," *IS-Seoul: Fifth International Symposium on Deformation Characteristics of Geomaterials*, Seoul, Korea, August 31-September 3, 6 pp.
- Fam, M., and Santamarina, J. C. (1997). "A study of consolidation using mechanical and electromagnetic waves." *Geotechnique*, 47(2), 203-219.
- Fernandez, A. L. (2000). "Tomographic Imaging the State of Stresses." PhD Dissertation, Georgia Institute of Technology, Atlanta.
- Hardin, B. O., and Richart, J., F.E. (1963). "Elastic wave velocities in granular soils." *ASCE -- Proceedings -- Journal of the Soil Mechanics and Foundations Division*, 89 33-65.
- Jacobson, D. E., Valdes, J. R., and Evans, T. M. (2007). "A numerical view into direct shear specimen size effects." *Geotech Test J*, 30(6), 512-516.
- Lee, J., and Santamarina, J. C. (2005). "Bender elements: Performance and signal interpretation." *J. Geotech. Geoenviron. Eng.*, 131(9), 1063-1070.
- Li, L., and Holt, R. M. (2002). "Particle scale reservoir mechanics." *Oil and Gas Science and Technology*, 57(5), 525-538.
- Montoya, M., Gerhard, R., DeJong, J., Weil, M., Martinez, B., and Pederson, L. (2012 (in press)). "Fabrication, Operation, and Health Monitoring of Bender Elements for Aggressive Environments." *Geotechnical Testing Journal*, 35(5), 1-15.
- O'Donovan, J., O'Sullivan, C., and Marketos, G. (2012). "Two-dimensional discrete element modelling of bender element tests on an idealised granular material." *Granular Matter* 14, 733-747.
- O'Sullivan, C. (2011). *Particulate discrete element modelling : a geomechanics perspective*. Taylor & Francis, London.
- Patel, A., Bartake, P. P., and Singh, D. N. (2009). "An empirical relationship for determining shear wave velocity in granular materials accounting for grain morphology." *Geotech Test J*, 32(1), 1-10.
- Sadd, M. H., Tai, Q., and Shukla, A. (1993). "Contact law effects on wave propagation in particulate materials using distinct element modeling." *Int. J. Non-Linear Mech.*, 28(2), 251-65.
- Sanchez-Salinero, I., Roesset, J. M., and Stokoe, K. H. (1986). "Analytical studies of body wave propagation and attenuation." *Rep. No. Report GR 86-15*, University of Texas, Austin.
- Santamarina, J. C. (2001). *Soils and waves : particulate materials behavior, characterization and process monitoring*. Wiley, New York.
- Styler, M. A., and Howie, J. A. (2012). "Comparing frequency and time domain interpretations of bender element shear wave velocities." *GeoCongress 2012*, ASCE, Oakland, CA, 2207-2216.
- Viggiani, G., and Atkinson, J. H. (1995). "Interpretation of bender element tests." *Geotechnique*, 45(1), 149-154.
- Yang, J., and Gu, X. Q. (2012). "Shear stiffness of granular material at small strains: does it depend on grain size." *Géotechnique*, in press.
- Zhao, X., and Evans, T. M. (2009). "Discrete simulations of laboratory loading conditions." *International Journal of Geomechanics*, 9(4), 169-178.